



Hydrophilic modification of PVDF membrane with solution bulk polymerization graft and separation performance of oil–water

Xiaojiao Yu^{a,*}, Wenqin Dai^a, Yingjuan Zhao^a, Liuyang Tang^a, Yuchen Wei^b, Binghua Yao^a

^aSchool of Science, Xi'an University of Technology, No.5 South Jinhua Road, Xi'an 710048, China, Tel./Fax: +86 29 82066360; emails: yxjw@xaut.edu.cn (X. Yu), 18792498485@139.com (W. Dai), 53091525@qq.com (Y. Zhao), tangliuyang108@163.com (L. Tang), bhyao@xaut.edu.cn (B. Yao)

^bSchool of Science, the Hong Kong University of Science and Technology, Clear Water Bay, Kowloon, Hong Kong, China, Tel. +00852 53449506; email: wych82313102@gmail.com (Y. Wei)

Received 5 March 2018; Accepted 13 July 2018

ABSTRACT

The surface of polyvinylidene fluoride (PVDF) membrane is modified with styrene and acetyl sulfate by the method of solution bulk polymerization graft, and polystyrene sulfonated (PSSA) grafted-modified membrane (PVDF-PSSA) is prepared. The surface structure and performance of PVDF-PSSA membrane are characterized and analyzed using scanning electron microscope, Fourier-transform infrared spectroscopy-attenuated total reflection, UV-visible spectrophotometer, X-ray photoelectron spectrophotometer, X-ray diffractometer, contact angle (CA), mercury porosimetry, thermogravimetric analyzer-differential thermal analysis and electronic tensile testing machine, respectively. The flux and separation performance of PVDF-PSSA membrane are studied. The results show that PVDF membrane surface occurs to have defluorination reaction so as to generate an unsaturated double bond through the alkali treatment. Styrene and sulfonic group are grafted to membrane surface. The modified membrane inherits α -phase crystalline phase, and the thermal decomposition temperature is over 300°C. The CA of modified membrane decreases from 114° to 33°. Both hydrophilicity and permeability are enhanced. The pure water flux of modified membrane increases compared with PVDF membrane, and rejection rate for diesel fuel can reach to 99.8%. The flux decline ratio of modified membrane reduces from 39.92% to 1.34%, and the flux recovery ratio increases from 60% to 84.87% after cleaning. The modified membranes exhibited enhanced stability, antifouling properties, and rejection rate, which can prove the potential of the membrane in petrochemical wastewater treatment.

Keywords: Polyvinylidene fluoride membrane; Surface modification; Performance; Oil–water separation

1. Introduction

Membrane technology created by multidisciplinary development over the past 30 years or so is a new water treatment technology. It not only purifies wastewater, but also recycles useful substances effectively. Compared with the traditional methods [1], membrane technology has had many advantages, such as low energy consumption, high single-stage separation efficiency, non-secondary pollution,

good selectivity, etc. It has found a wide application in the field of wastewater treatment, food hygiene, environmental protection, and other processes. Polyvinylidene fluoride (PVDF) membrane is considered to be one of the most attractive polymer materials in membrane technology. It exhibits more excellent characteristics with better thermal stability, chemical resistance, and mechanical properties [2]. For this reason, it has been widely used in ultrafiltration, microfiltration, gas separation, and wastewater treatment. Although

* Corresponding author.

the PVDF membrane exhibits excellent performance, it has had a big membrane permeability resistance and low water flux. In the oil/water separation process, the organic matter, protein, and others are readily adsorbed on the membrane surface, thus causing serious membrane fouling pores. The membrane flux can be greatly attenuated, and service life is reduced. These can restrict application of PVDF in the field of membrane separation greatly [3]. Therefore, modification of PVDF membrane is important, and it has received extensive attention from a majority of researchers.

Many studies show that an increase in hydrophilicity will help promote membrane permeability performance and effectively reduce membrane fouling [4–8]. There are many methods to modify hydrophilic of PVDF membrane including body modification and surface modification [9,10]. Owing to poor compatibility of the modified material, the physical properties of modification membrane was reduced after body modification [11–13], thus limiting the scope of application. The surface modification could not only maintain good physical properties of PVDF membrane, but also endow the surface with new properties [14–17]. PVDF membrane after being grafted can be widely used because of its good mechanical properties and special functional groups on the surface of the materials. Although graft modification has had many advantages, water flux decreases distinctly after graft modified [18,19]. Rahimpour et al. [20] have modified PVDF membrane by UV photografting of hydrophilic monomers. The study has found that pure water flux of all modified membranes is decreased. Some approaches of PVDF membrane surface hydrophilic modifications have been used to optimize the membrane performance [21,22], but more effective methods need to be developed to further improve membrane antifouling properties and oil/water separation performance. Due to the desirable hydrophilicity, styrene sulfonate is considered as an attractive additive for graft modification of PVDF membrane, most of them adopt body modification [23,24]. The modified membranes have been intensively investigated in the application of direct methanol fuel cell [25,26], and there is less research on oil/water separation performance. Therefore, the research modified of PVDF membrane using styrene sulfonic acid as additive is necessary.

The aim of this paper is not only to make PVDF modification membrane to maintain excellent performance, but also to improve membrane fouling resistance, hydrophilic, pure water flux, and oil/water separation performance. Styrene and acetyl sulfate as additive is proposed to modify PVDF membrane using surface graft method, and the PVDF-polystyrene sulfonated (PSSA)-modified membrane has been prepared. The structure and properties of modified membrane are studied. Oil/water separation performance of PVDF-PSSA-modified membrane is discussed with ideal experimental results obtained.

2. Experiment

2.1. Materials

Hexadecyl trimethyl ammonium bromide (CTMAB) was purchased from BASF Chemical Co., Ltd. (Tianjin, China). Phenylethene was obtained from ChengDu Kelong Chemical Co., Ltd (Chengdu, China). Benzoyl peroxide (BPO) was

supplied by Kemiou Chemical Reagent Co., Ltd. (Tianjin, China). Alkylphenol ethoxylates (OP-10) was purchased from Shan Pu Chemical Co., Ltd. (Shanghai, China). Diesel oil was obtained from Sinopec Co., Ltd (Xian, China). The PVDF membrane was supplied by Shanghai Diqing Filtering Technology Co., Ltd. (China, film thickness 65 μm and porosity 75%).

2.2. Experimental mechanism

The chemical equation of PVDF membrane surface modifying is shown in Fig. 1. First, in strong alkali oxidation system or strong alkali phase-transfer catalytic system, hydrogen fluoride was removed from PVDF membrane and generated carbon-carbon double bond [27,28]. Then, under the action of the initiator BPO, it reacted free radical polymerization (P) with styrene (S) and produced the copolymer of PVDF membrane and styrene (PVDF-PS). The PVDF-PS reacted sulfonation reaction with fresh acetyl sulfate and generated the sulfonated styrene grafted membrane (PVDF-PSSA) eventually.

2.3. Alkali treatment of PVDF membrane

PVDF membrane was infiltrated in ethanol for 10 min, taken out for washing with deionized water, dried at 30°C, and then it was put into the solution consisting of 3.0 mol/L of KOH and 5.0% of KMnO_4 (referred as System 1). The reaction time was 3 h under the condition of 80°C water bath, and then the PVDF membrane was taken out for washing with deionized water until washing deionized water became neutral. As a result, the PVDF-1 membrane was obtained. Another dried PVDF membrane was placed in the solution consisting of 1.0 mg/mL of phase-transfer catalyst CTAB and 3.0 mol/L of NaOH (referred as System 2). The reaction time was 2 h under the condition of 60°C water bath, the PVDF membrane was taken out for washing with deionized water until washing deionized water became neutral, as a result, the PVDF-2 membrane was obtained.

2.4. Preparation of PVDF-PSSA membrane

A total of 15.0 mL of acetic anhydride was added to an equal volume of 1,2-dichloroethane (DCE) at 5°C and stirred well. When the temperature dropped to 5°C, 10.0 mL of concentrated sulfuric acid was added dropwise, and then reacted for 30 min. The fresh acetyl sulfate was prepared after rapid stirring 10 min, and then set aside.

In total, 0.3 g of BPO was added into 100.0 mL of the mixed solution consisting of styrene and tetrahydrofuran (referred

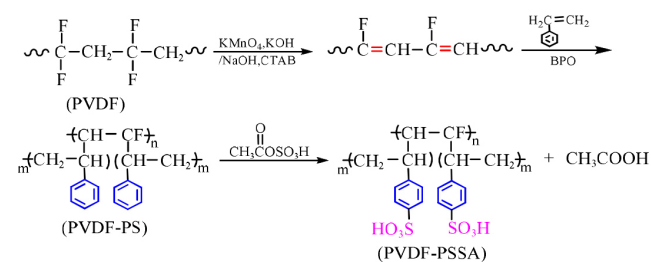


Fig. 1. The chemical equation of PVDF membrane surface modifying.

as Solution A). The volume ratio of styrene and tetrahydrofuran was 5:1. Under the protection of nitrogen, PVDF-1 membrane reacted with Solution A in 78°C water bath for 12 h to obtain a PVDF-PS-1 membrane. The PVDF-PS-1 membrane was swelled for 2 h under 70°C in DCE. And then it was put into the fresh acetyl sulfate solution, and reaction time was 4 h under the condition of 70°C. The PVDF-PSSA-1 membrane was obtained. The PVDF-2 membrane was used to prepare the PVDF-PSSA-2 membrane in terms of the above steps, so as to obtain the PVDF-PSSA-2 membrane.

2.5. Structural characterization of PVDF-PSSA membranes

The surface and cross-sectional morphology of the PVDF-PSSA membranes were observed with a field emission scanning electron microscope (SEM, JSM-6700F, Japan). The membrane was immersed in ethanol for 5 min, put into liquid nitrogen for about 2–3 min, and then it was taken out for fracturing. The sample was positioned on a metal holder, then sputter coated with gold under vacuum for 5 min before testing. The pore size of the membrane was determined by mercury porosimetry (AutoPore IV9500, Micromeritics, USA), the equilibration time was 10 s, and maximum intrusion volume was 1.000 mL/g. The surface functional groups of modified membrane were analyzed using IRAffinity-1-type Fourier transform infrared spectroscopy (FTIR-ATR, Shimadzu, Japan). Instrument resolution was 4.0, and the scanning was in a wavelength range of 650–4,000 cm^{-1} . The characteristic functional groups of modified membrane surface were investigated using UV-3600 type UV-visible spectrophotometer (UV-Vis, Shimadzu, Japan) with PVDF membrane as reference. X-ray photoelectron spectrophotometer (XPS) spectra for the element composition and chemical bond of modified membrane surface were recorded on a K-Alpha X-ray photoelectron spectrophotometer (Thermo, Britain) employing Al Ka excitation radiation ($h\nu = 1,486.6 \text{ eV}$). XRD-7000-type X-ray diffractometer (XRD, Shimadzu, Japan) was used to analyze the crystal structure of modified membrane employing $\text{CuK}\alpha$ radiation and a scanning speed of $4^\circ/\text{min}$. The hydrophobicity of PVDF-PSSA-modified membrane was studied based on the contact angle (CA) by OCA20-type of contact angle measuring instrument (Dataphysics, Germany). The contact time of each sample with the droplet was 5 s by the pendant drop method, and each sample was measured for five times with average value taken to minimize the experimental error. A thermogravimetric analysis was conducted to study the thermal stability of the membranes using a DTG-60AH thermogravimetric analyzer (TGA-DTA, Shimadzu, Japan). The samples were heated to 1,000°C at a heating rate of 20°C/min. The mechanical property of modified membrane was determined according to literature [29]. The properties of simulated diesel wastewater (such as mean particle diameter, particle size distribution) were measured using Delsa™ nano C particle analyzer (Beckman coulter, Inc., USA) at 25°C with accumulation times 30 s.

2.6. Preparation of simulated diesel wastewater

A total of 1.0 mg alkylphenol polyoxyethylene ether (OP-10) was added to 100.0 mg 0# diesel oil ($\rho = 0.835 \text{ g/mL}$)

with ultrasonic oscillation for 10 min. Then, it was diluted with water to 1.0 L with continuous ultrasonic oscillation for 1 h, so that simulated diesel wastewater solution of 100.0 mg/L was obtained. The particle size distribution of simulated diesel wastewater is shown in Fig. 2. As indicated in Fig. 2, the particle diameter of simulated diesel wastewater was mainly distributed in 435–665 nm. And the mean particle diameter was 638.6 nm.

2.7. Membrane flux measurement

A self-made dynamic circulation membrane performance experimental setup [29] was used to measure membrane flux. The absolute pressure of the system was adjusted to 125.02 KPa after preloading 40 min under the pressure of 145.02 KPa. The pure water and simulation diesel wastewater (100.0 mg/L) were filtered with the stirring rate of 500 rpm, respectively. Then the membrane was rinsed with deionized water and ultrasonic concussion 10 min, and the flux recovery was recorded. The volume of the effluent liquid was measured at an interval of every 10 min. The membrane flux (J), flux decline ratio (FDR), and flux recovery ratio (FRR) were calculated using Eqs. (1)–(3) [30], respectively. And the effective membrane area was $1.32 \times 10^{-3} \text{ m}^2$.

$$J = \frac{V}{A\Delta t} \quad (1)$$

$$\text{FDR}(\%) = \frac{J_1 - J_2}{J_1} \times 100 \quad (2)$$

$$\text{FRR}(\%) = \frac{J_{wc}}{J_{wo}} \times 100 \quad (3)$$

where V is the volume of the effluent (L), A is effective membrane area (m^2), t is effluent time (h), J_1 is starting flux of simulation diesel wastewater, J_2 is last flux of simulation diesel wastewater, J_{wo} is pure water flux of the new membrane, and J_{wc} is pure water flux of the membrane after cleaning.

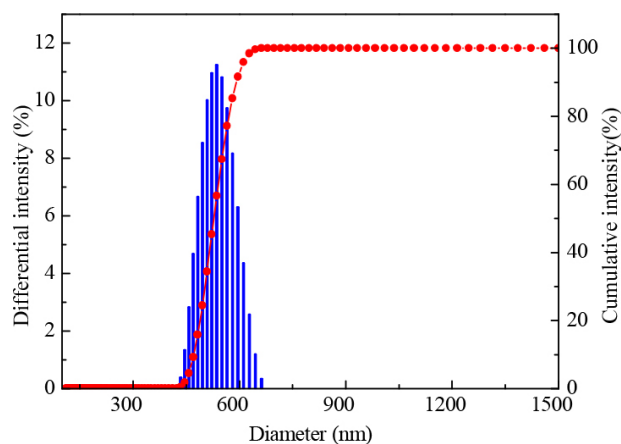


Fig. 2. The particle size distribution of simulated diesel wastewater.

2.8. Rejection rate measurement of PVDF-PSSA membranes

The simulation diesel wastewater was disposed at the absolute pressure of 125.02 KPa with the stirring rate of 500 rpm. The measurement was carried out in the experimental setup of literature [29]. Diesel concentration was determined by UV-spectrophotometer at the wavelength of 224 nm. The rejection rate of the membrane was calculated according to Eq. (4) [30].

$$R = \frac{C_{\text{feed}} - C_{\text{perm}}}{C_{\text{feed}}} \times 100\% \quad (4)$$

where R is rejection rate (%); C_{feed} is diesel concentration in the feed phase (mg/L), and C_{perm} is diesel concentration in the permeated liquid (mg/L).

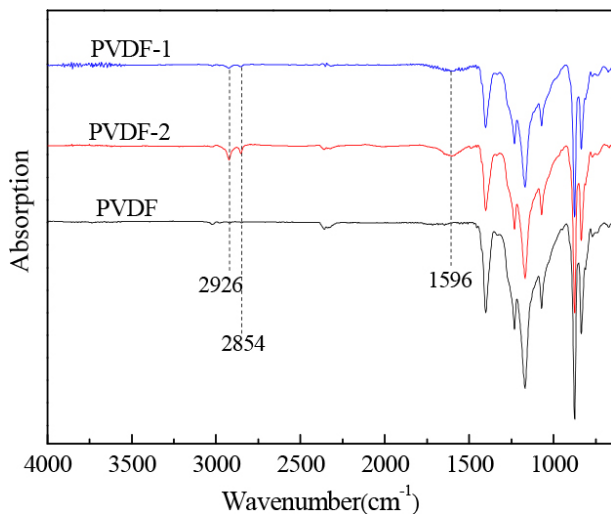


Fig. 3. FTIR-ATR spectra of alkaline-treated PVDF membrane.

3. Results and discussion

3.1. FTIR-attenuated total reflection (ATR) and UV-Vis analysis

The FTIR-ATR spectra of PVDF membrane by the alkaline treatment is shown in Fig. 3. The PVDF-1 and PVDF-2 show characteristic bands at 1,596 cm^{-1} (characteristic of $\sim\text{C}=\text{C}=\text{C}\sim$ backbone carbon-carbon double bond stretching vibration), 2,926 cm^{-1} and 2,854 cm^{-1} (symmetric and asymmetric C-H stretch). These indicate that carbon-carbon double bonds are formed on the surface of PVDF membrane through defluorination reaction. Furthermore, the peak intensity of the PVDF-2 membrane is larger than PVDF-1 membrane. It can be explained that a phase-transfer catalyst system can result in obvious changes in molecular structure of PVDF membrane surface so that more carbon double bonds are formed.

The FTIR-ATR spectra of modified membrane are shown in Fig. 4. Four characteristic peaks of PVDF are observed in the spectra of all membranes at 1,406 cm^{-1} (C-H bending of methylene stretching vibration), 1,169 cm^{-1} (C-C stretching vibration), 1,230 cm^{-1} , and 1,070 cm^{-1} (C-F stretching vibration). The peak intensity of the PVDF-PSSA-2 membrane is larger than PVDF-PSSA-1 membrane. Compared with the spectrum of the PVDF membrane, new peaks appear at 3,443 cm^{-1} and 1,682 cm^{-1} in the spectra of modified membrane. They are attributed to the characteristic absorption peaks of $-\text{SO}_3\text{H}\cdot\text{H}_2\text{O}$ and benzene skeleton vibration. In addition, some other new peaks are also observed, being ascribed to the characteristic peaks of hydrogen on benzene ring at 672 cm^{-1} , characteristic of para-substituted benzene peak at 1,032 cm^{-1} and 1,124 cm^{-1} , and S-O of $-\text{SO}_3\text{H}$ symmetric stretching vibration characteristic peaks at 1,004 cm^{-1} in the spectra of modified membrane. These results indicate that the styrene is grafted onto the PVDF membrane surface and a sulfonic acid group is introduced into the para position of the benzene ring.

Fig. 5 is UV-Vis spectra of the modified membrane. It can be seen from Fig. 5 that a B-band absorption peak with moderate intensity appears at 200–300 nm, and the peak shape is

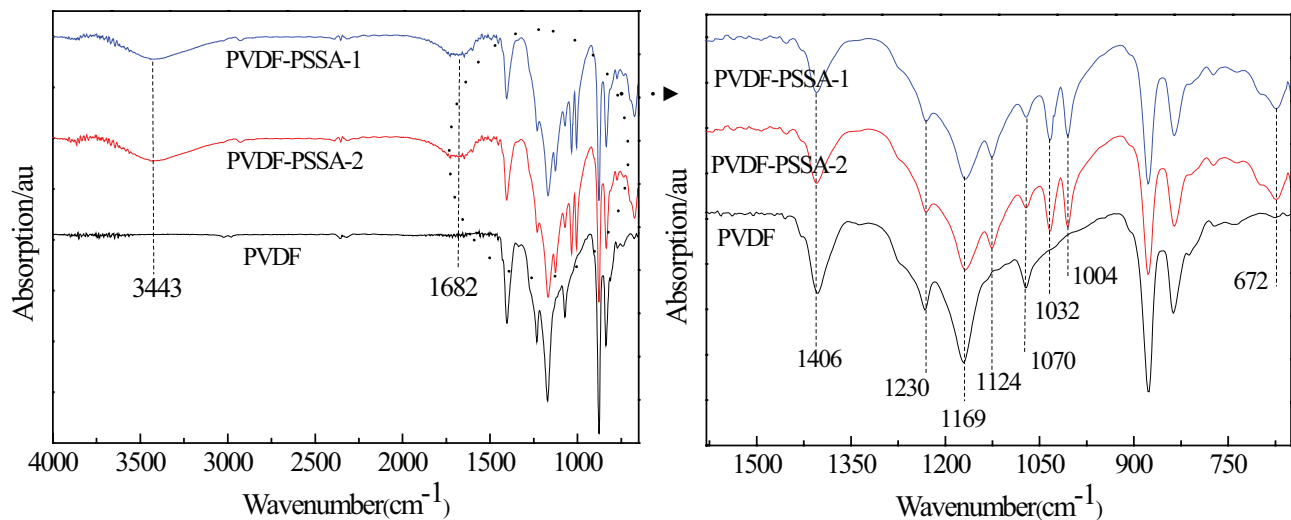


Fig. 4. FTIR-ATR spectra of PVDF and modified membrane.

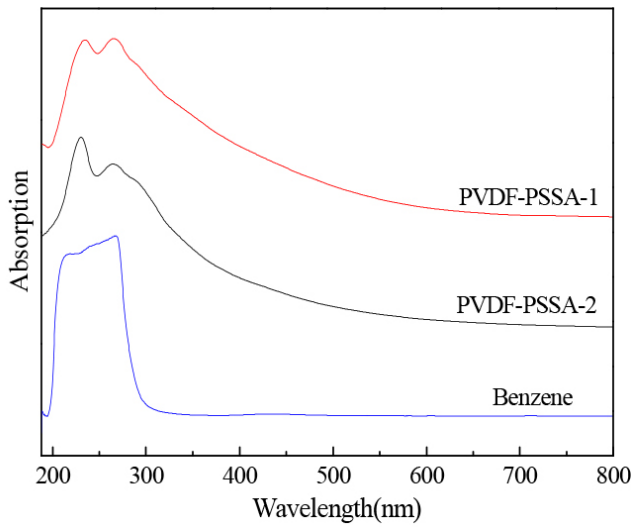


Fig. 5. UV-Vis spectra of modified membrane.

similar to the conjugate characteristic absorption peak of a benzene ring. It indicates that there is a benzene ring on the modified membrane. A bimodal appears near 250 nm, which may be due to the influence of the introduction of sulfonic acid groups.

3.2. XPS analysis

The XPS spectra of the membrane are shown in Fig. 6. Fig. 6(a) shows that the peaks at binding energy (BE) of 284.6 eV, 688 eV, 833.08 eV, and 1,228 eV correspond to C1s, F1s, auger peak of F, and auger peak of C, respectively. Also, the peak at BE of 168.5 eV, 532.5 eV, and 979.1 eV are associated with S2p, O1s, and auger peak of O, respectively. It indicates that S and O elements are combined with PVDF membrane in some chemical bonds. In Fig. 6(b) for the spectrum of C1s, there are two peaks at 290.1 eV and 286.6 eV corresponding to the BE of C–F₂ and C–H₂ and the two peak areas are 11,346.68 and 12,967.61, respectively. The two peak area ratios are closed to 1:1. This indicates that the C–F and C–H

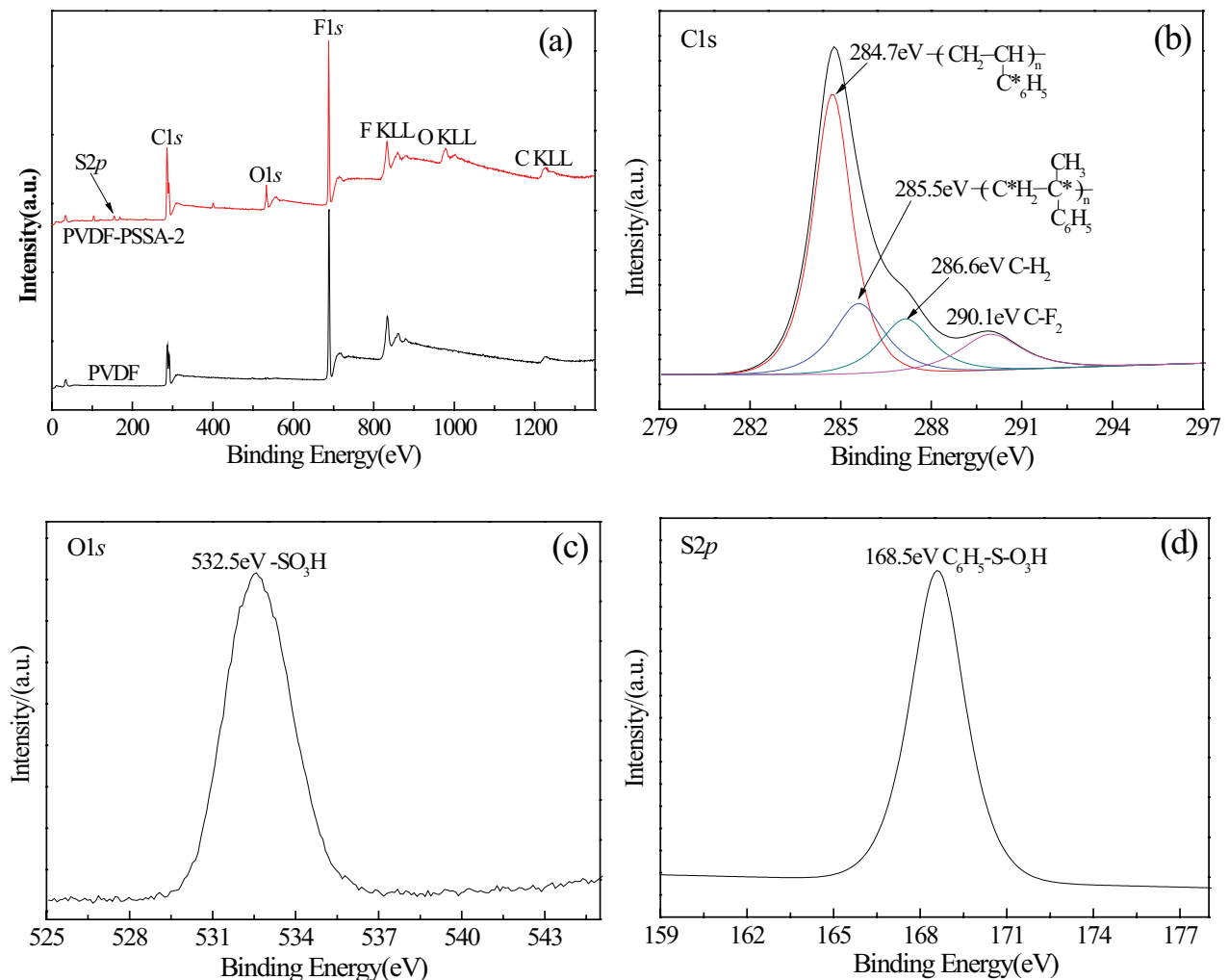


Fig. 6. XPS spectra of modified membrane: (a) the survey spectra of modified membrane and PVDF membrane, (b) C1s spectra, (c) O1s spectra, and (d) S2p spectra.

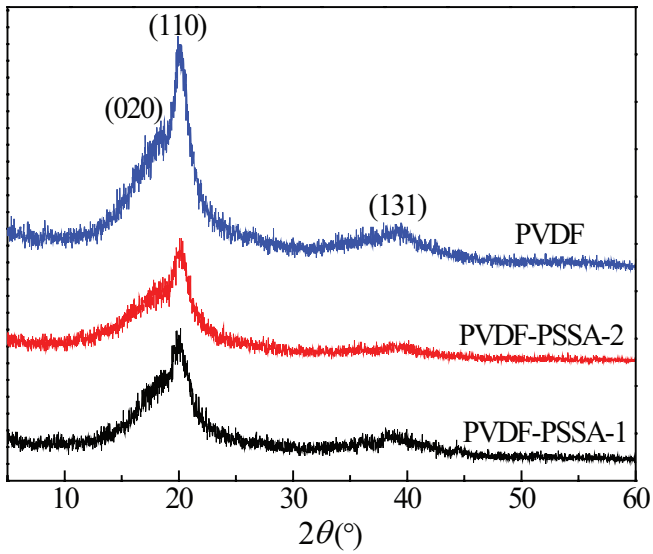


Fig. 7. XRD patterns of PVDF and modified membrane.

bands on the PVDF membrane surface are broken simultaneously. The peaks at 284.7 eV and 285.5 eV belong to C1s of the benzene ring and $(-C^*H_2-C^*(CH_3)(C_6H_5))_n$, respectively. This suggests that the F or H of modified membrane surface should be replaced by polystyrene group, and that the polystyrene groups are combined with PVDF membrane by chemical bonds. Fig. 6(c) shows that characteristic peak appears at 532.5 eV corresponding to the BE of O1s in sulfonic group. And the peak area is 6,094.96. In the Fig. 6(d), $S2p_{3/2}$ peak is located at 168.5 eV corresponding to S–O BE in toluenesulfonic acid. The area of peak was calculated as 1,780.00. The peak area ratio of $S2p_{3/2}$ and O1s is approximately 1:3, whereby further inferring that there might exist O and S as a sulfonic group.

3.3. XRD analysis

The XRD patterns of the membranes are provided in Fig. 7. As can be seen from Fig. 7, the PVDF membrane shows that there are three perceptible peaks at 2θ value 18.54° , 19.89° , and 39.4° . These are typical α -phase PVDF characteristics peaks. They correspond to (020), (110), and (131) diffraction

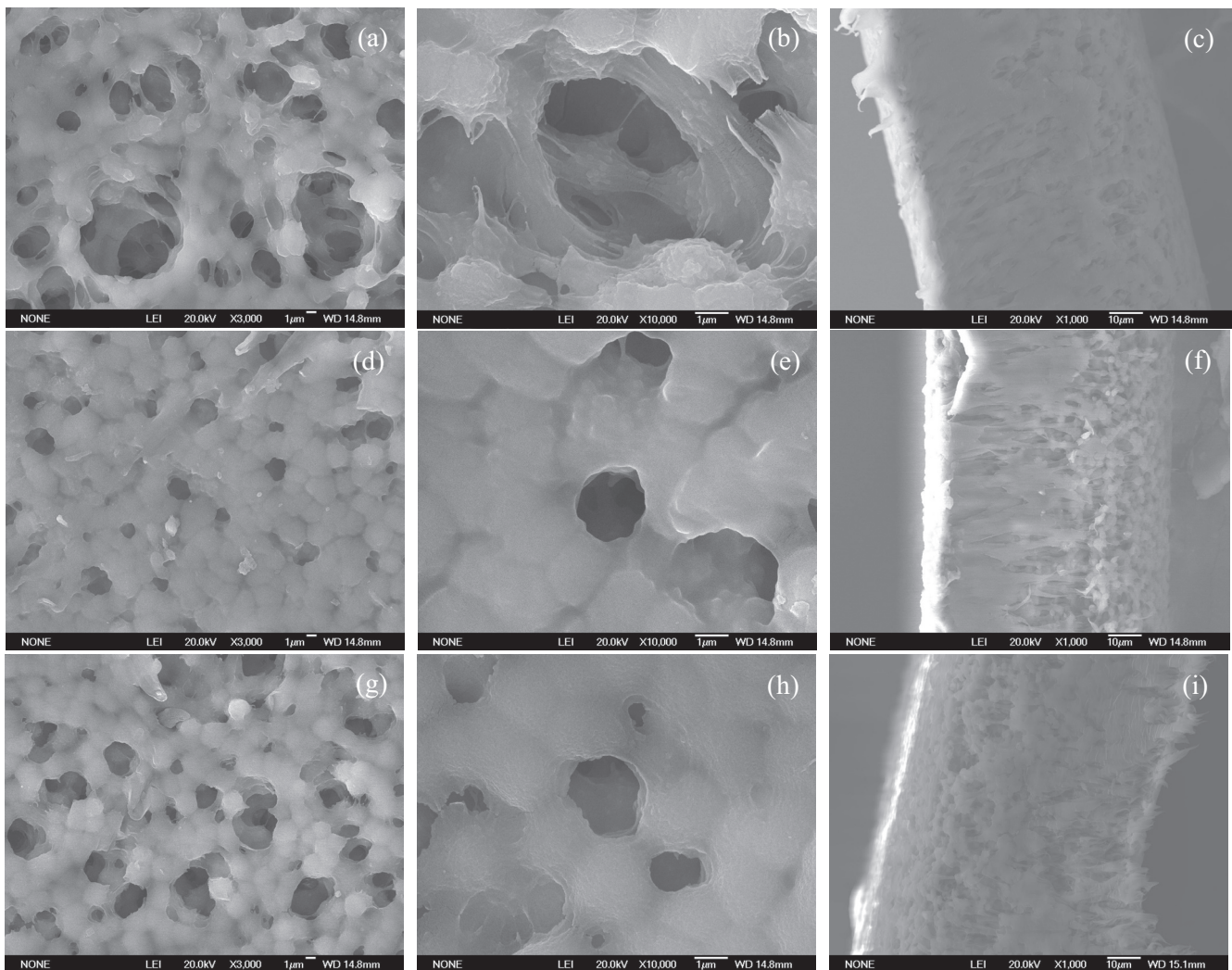


Fig. 8. SEM images of the membrane: (a)–(c) PVDF membrane; (d)–(f) PVDF-PSSA-2 membrane; (g)–(i) PVDF-PSSA-1 membrane.

planes of the crystalline region, respectively [31]. The (110) planes of the crystalline region of PVDF-PSSA-1 and PVDF-PSSA-2 membrane do not change significantly, whereby indicating that the modified membrane retains the α -phase of the original film. It can be seen from Fig. 8 that the intensity of the sharp PVDF peaks decreases and peak shape is passivated. This may be due to the breakage of strong polarity of C–F bond, so that the crystallinity of PVDF decreases. The crystal structure transforms the ordered state into the disordered state, and amorphous region of the membrane is increased. Therefore, we can say that amorphous region of the membrane increases by surface modification but does not damage the original crystalline phase. The PVDF-PSSA membrane remains the original crystal characteristics of PVDF membrane.

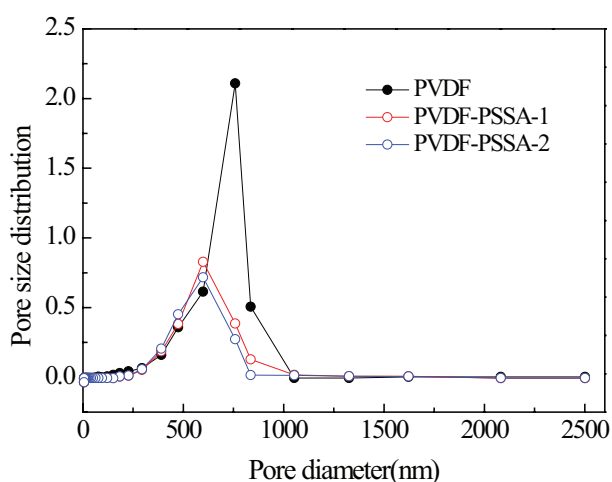


Fig. 9. The pore size distribution of PVDF and modified membrane.

3.4. SEM analysis

Fig. 8 indicates SEM images of the membranes. Albo et al. [32,33] reported that the separation characteristics of the membranes were mainly attributed to two different structures, which is a dense matrix and highly permeable regions of the membrane. Fig. 8 shows that the PVDF-PSSA membrane has had two different structures. First, there are cross-linked structure holes that can increase the apparent retention rate. Second, there are finger holes indicating where there are highly permeable regions. The structure is similar to the above reports in the literature, and there should be good separation performance. Figs. 8(d) and (g) show that there is an obvious polymer layer on the surface of PVDF-PSSA membrane. PVDF-PSSA-2 membrane surface is relatively flat, and the pore size is smaller than that of PVDF membrane. Fig. 9 shows the pore size distribution of PVDF and modified membrane. As depicted in Fig. 9, the modified membrane shows smaller pore size than the PVDF membrane. The median pore diameter of PVDF, PVDF-PSSA-1, and PVDF-PSSA-2 membranes is 786.8, 652.3, and 612.2 nm, respectively. This is helpful to improve the membrane rejection rate. It can be seen from Figs. 8(e) and (h) that the through hole structure of PVDF-PSSA-2 membrane surface is more obvious, and PVDF-PSSA-1 membrane surface is crosslinked structure hole. Moreover, the cross-sectional images Figs. 8(c), (f), and (i) show that the sub-layer of PVDF-PSSA-2-modified membrane maintains finger hole structure of PVDF membrane which can improve permeability of the membrane. It is due to the phase-transfer catalyst accelerating the phase transfer speed, and conducive to the formed finger macropores. It could reduce the permeability-resistance of PVDF-PSSA-2 membrane and increase permeability. Therefore, the System 2 is much more conducive to hydrophilic modification of PVDF membrane.

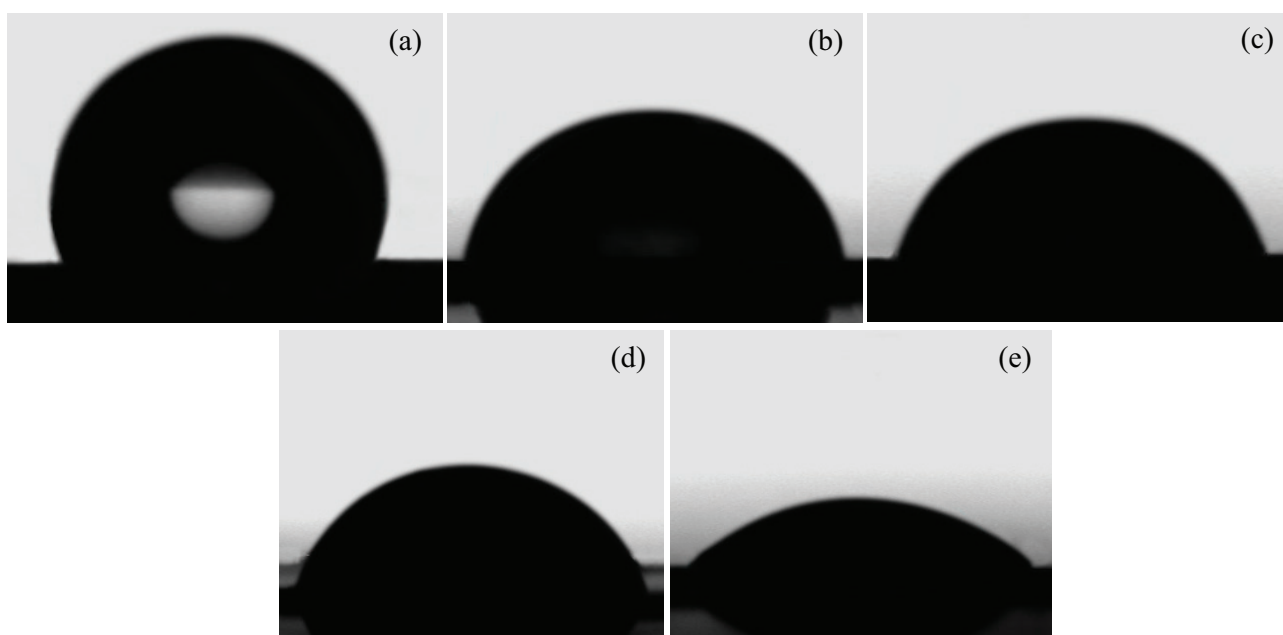


Fig. 10. The contact angle images of the membrane: (a) PVDF membrane, (b) PVDF-1 membrane, (c) PVDF-2 membrane, (d) PVDF-PSSA-1 membrane, and (e) PVDF-PSSA-2 membrane.

3.5. Hydrophilicity and permeability analysis

Fig. 10 shows the CA of membrane. The CA of PVDF-1 and PVDF-2 membranes are dropped from 114° to 78°, and 72°, respectively. This is because that the strong hydrophobic group (-F) is taken off, and the hydrophilicity of the

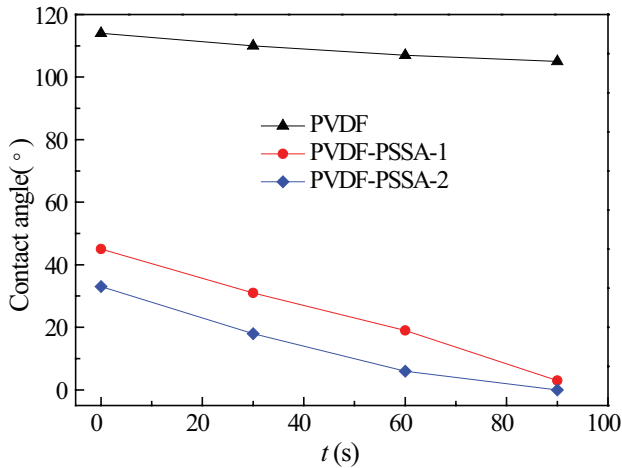


Fig. 11. The curve for contact angle change over time.

membrane surface is enhanced. The CAs of PVDF-PSSA-1 and PVDF-PSSA-2 membranes are 45° and 33°, respectively. It is suggested that the hydrophilicity of PVDF-PSSA membrane should be improved significantly. This is because that the hydrophilic groups -SO₃H are introduced to the membrane surface. The more hydrophilic groups are grafted to the membrane surface, the greater hydrophilicity will be and the smaller CA of membrane will become. Therefore, grafting rate of -SO₃H in the System 2 is higher than that of the System 1, and System 2 is much more conducive to the hydrophilic modification of membrane.

The curve for CA change over time is shown in Fig. 11. It can be drawn from Fig. 11 that the CA of modified membrane decreases with an increase in time, and that the membrane is completely infiltrated with water at 90 s. There is almost no change in the CA of PVDF membrane in 90 s. This indicates that water is gathered on PVDF-PSSA membrane surface by -SO₃H, so as to promote water to diffuse into the membrane matrix, and enhance the permeability of the membrane [34].

3.6. Thermal stability analysis

Thermal properties of modified membrane are studied by TGA-differential thermal analysis (DTA), as shown in Fig. 12. Fig. 12 shows that the endothermic peak of all samples appears

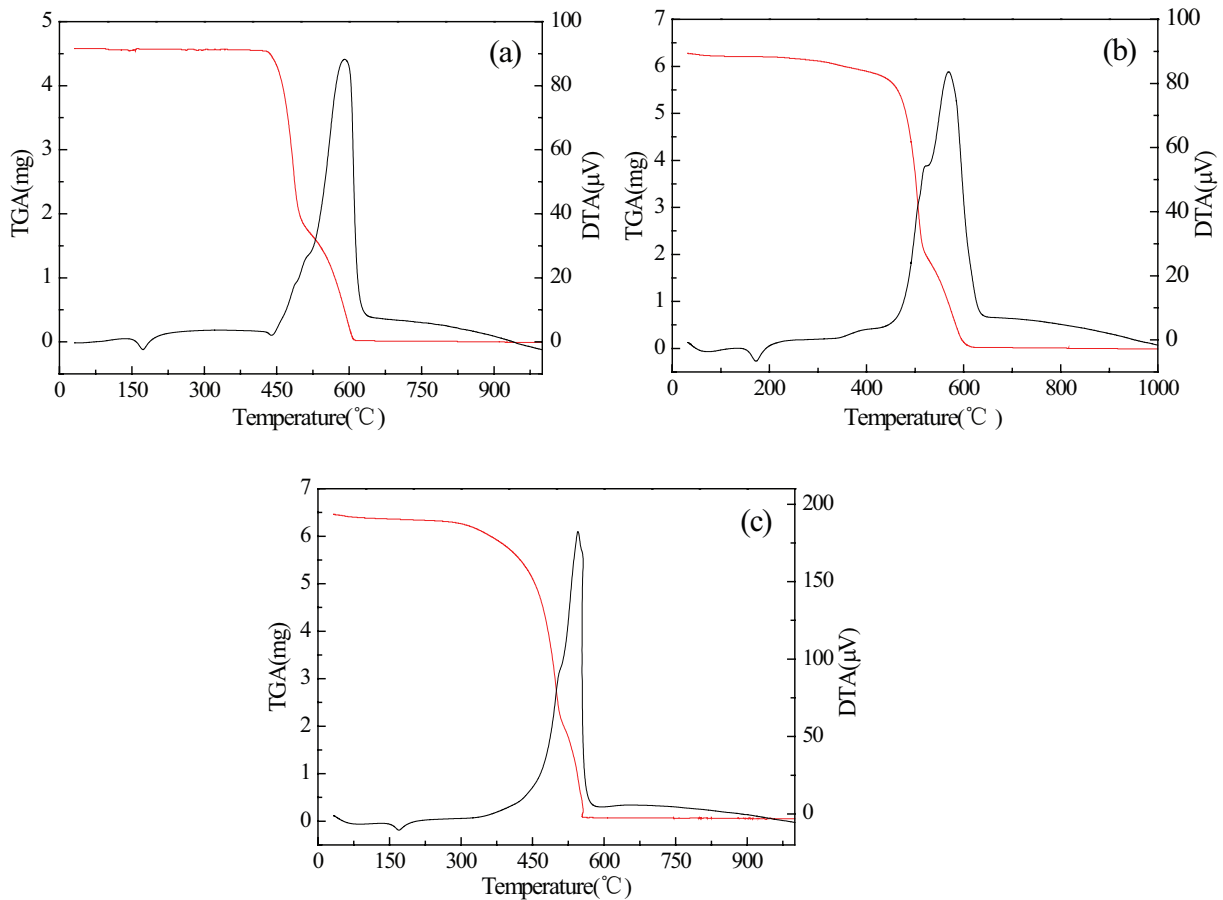


Fig. 12. TGA-DTA graph of the membrane: (a) PVDF membrane, (b) PVDF-PSSA-1 membrane, and (c) PVDF-PSSA-2 membrane.

at 172.9°C in the curve of DTA, it is caused by loss of bound water in PVDF membrane [35]. Only one-step weight loss pattern can be observed from Fig. 12(a). PVDF membrane begins to decompose at 463 °C, completely decomposed at 607°C, and the final decomposition rate is 99.46%. Both of PVDF-PSSA-1 and PVDF-PSSA-2 membrane exhibit two similar weight loss processes in Figs. 12(b) and (c). The first stage of slow decomposition appears between 300°C and 450°C, and the decomposition rate is about 20%. It is attributed to the decomposition of sulfonic acid groups [36,37]. The second stage of rapid decomposition occurs between 450°C and 600°C, completely decomposes at about 607°C, and the final decomposition rate is more than 98%. It is consistent with the weight loss curve of PVDF membrane; therefore it corresponds to the decomposition of PVDF polymer chain. It is suggested that the thermal stability of modified membrane is influenced by hydrophilic modification. However, the modified membrane still remains a good thermal stability, because the thermal decomposition temperature is over 300°C, and it can satisfy the application requirements.

3.7. Mechanical property analysis

Stress–strain tests results are presented in Fig. 13. The figure shows that the influence of pre-treatments and surface modification upon mechanical properties of the membrane is very significant. After surface modification, the tensile strength of PVDF-PSSA-1 and PVDF-PSSA-2 are decreased from 15.93 to 10.45, and 12.44 MPa, respectively. Also, the strain at break of PVDF-PSSA-1 and PVDF-PSSA-2 significantly decreases from 39.00% to 22.57%, and 30.55%, respectively. This implies that the elastic property or flexibility is weaker after surface modification. It has been proposed that mechanical properties changes are due fundamentally to the reactions between the chemical reagents and the membrane's some specific functional groups [38]. According to the literature [39], the reduction in mechanical properties of modified membrane is linked to the chain breaking of membrane materials. Chain breaking on membrane polymer influences continuing deterioration of the membrane layer and as a result, the interaction between polymer molecules is weakened and becomes easier to fracture. Particularly for PVDF, it is believed that the reduction in

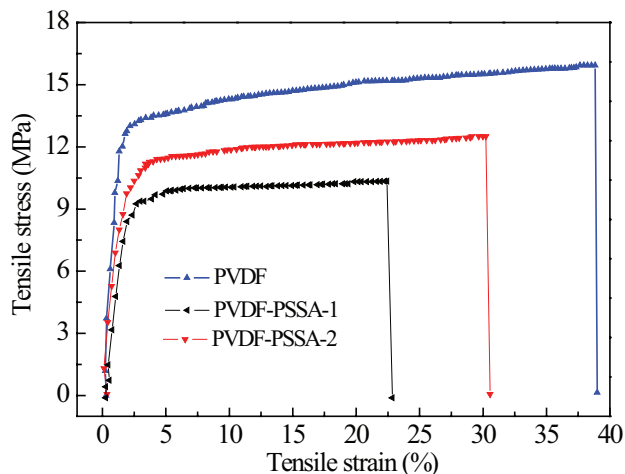


Fig. 13. Stress–strain plots of the membrane.

the membrane's mechanical properties after the NaOH treatment could be due to the chemical reaction between PVDF and NaOH [40]. The reduction in mechanical properties of modified membrane is attributed to the dehydrofluorination reaction. This is consistent with the FTIR-ATR and XPS analysis results. It can be seen from Fig. 13 that the tensile strength and strain at break of PVDF-PSSA-2 is better than PVDF-PSSA-1. This indicates that the pre-treatment through the System 1 has had a greater bearing on the mechanical properties of membrane. It may be due to phase-transfer catalysts are added to System 2 in the pre-treatment process. As a consequence, the reaction on the surface of the membrane is more homogeneous. Thus the mechanical properties of PVDF-PSSA-2 membrane are reduced slightly compared with PVDF-PSSA-1 membrane.

3.8. Membrane flux analysis

The flux curve of the membrane is shown in Fig. 14. As can be seen from Fig. 14, the pure water flux of PVDF, PVDF-PSSA-1, and PVDF-PSSA-2 membrane are 210.0, 391.1, and 464.5 L/(m²·h), respectively. Simulation diesel wastewater was disposed after 60 min, the membrane flux decreased to 77.2, 201.4, and 242.2 L/(m²·h) from 128.5, 243.3, and 279.6 L/(m²·h), respectively. After cleaning, pure water flux of the membrane recovered to 126, 312.6, and 394.2 L/(m²·h), respectively. The pure water flux of PVDF-PSSA-1 and PVDF-PSSA-2 membrane increase significantly compared with the PVDF membrane. According to Eqs. (2) and (3), the FDR of PVDF, PVDF-PSSA-1, and PVDF-PSSA-2 membranes are 39.92%, 1.72%, and 1.34%, respectively, and the FRR are 60%, 79.92%, and 84.87%, respectively. It indicates that the pure water flux of modified membrane increase significantly compared with the PVDF membrane. Through surface modification, the FDR of membrane reduces after fouling and FRR increases after cleaning. The modified membranes showed relatively better stability performance and antifouling properties than those of unmodified membrane. This is because the sulfonic acid group is grafted on the PVDF membrane surface to enhance the hydrophilicity of membrane surface, which is in good agreement with the CA measurement in Fig.10 and SEM measurement in Fig. 8. The enhancement of surface

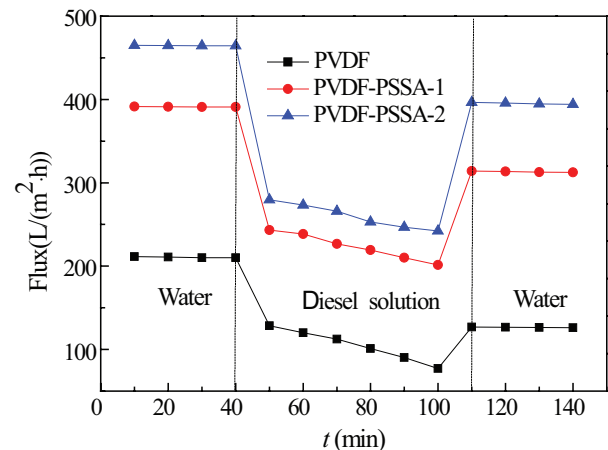


Fig. 14. The flux curve of the membrane before and after modification.

hydrophilicity is advantageous to reduction of the permeation resistance and improvement of antifouling performance [32,41,42]. The surface charge of PVDF-modified membrane is negative after grafting PSSA. The hydrophilic layer can be formed on the membrane surface due to the electrostatic and hydrogen-bonding interactions between water molecules and sulfonic acid group. This also is helpful for increasing FRR and improving antifouling properties of modified membrane [43,44].

3.9. The rejection rate analysis

The equilibrium curve of the membrane for intercept simulated diesel wastewater is shown in Fig. 15. As can be seen from Fig. 15, the diesel concentration of the treated water sample by PVDF membrane is higher than 60.02 mg/L, but treated by modified membrane is 6.15 mg/L. The rejection rates of PVDF-PSSA-2 and PVDF-PSSA-1-modified membrane and PVDF membrane for simulated diesel wastewater are calculated using Eq. (4). They are 99.8%, 93.9%, and 40.0%, respectively. The rejection rate of PVDF-PSSA-2 film is as high as 2.45 times of the PVDF membrane. The modified membrane exhibited higher rejection rates compared with the PVDF membranes. It may be due to the modified membrane PVDF-PSSA has smaller pores [45,46] and better hydrophilicity compared with the PVDF membrane [47]. According to the literature [48–50], the separation of oil/water by hydrophilic ultrafiltration membrane followed the membrane phase-separation mechanism. The separation mechanism is mainly attributed to the concentration polarization of water on the membrane surface during a membrane phase-separation process. Due to the membrane is hydrophilic, oil is difficult to get close to the membrane surface, thus the concentration of oil is lower when the distance from membrane surface is smaller, and the pure water layer is formed near the membrane surface. As the hydrophilicity of the membrane increases, the thickness of the pure water layer may increase, thus is able to block larger pores. The diffusion of water in the membrane matrix was promoted. It is also helpful to improve the rejection rates of membrane. It means that PVDF-PSSA-2-modified membrane can effectively separate oil/water of wastewater [51].

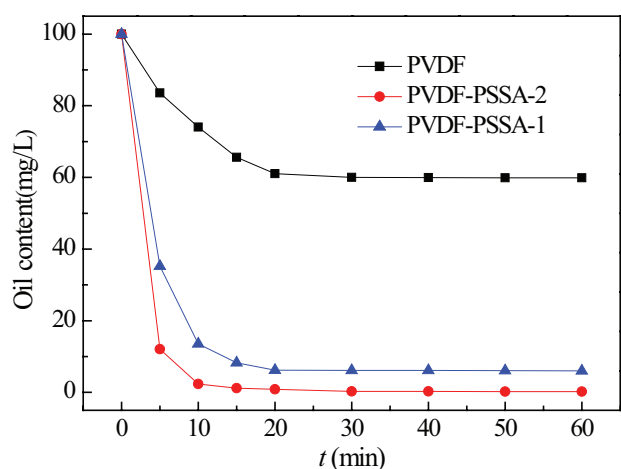


Fig. 15. The equilibrium curve of the membrane to intercept simulated diesel wastewater.

4. Conclusion

In this study, preparation, structure characterization, and performance of PVDF-PSSA membrane are investigated and the following conclusions can be obtained:

Styrene monomer and sulfonic group are grafted to PVDF-PSSA membrane surface. The polystyrene groups are combined with PVDF membrane by chemical bonds. The modified membrane can maintain finger hole structure of PVDF membrane and the pore size decreases compared with PVDF membrane. The hydrophilicity and permeability increase greatly. The mechanical properties of the membrane become weak after modification. The modified membrane has inherited good crystalline and thermal stability characteristics from PVDF membrane. The alkali phase-transfer catalyst system is much more conducive to the hydrophilic modification of PVDF membrane. The pure water flux of modified membrane increases and rejection rate for diesel fuel can achieve 99.8%. Compared with PVDF membrane, the modified membranes exhibited relatively better stability and antifouling properties than PVDF membrane.

Acknowledgments

This work was supported by the National Science Foundation of China (Nos. 21276208 and 21576220), the Natural Science Foundation of Shaanxi Province (No. 2015JZ005), and the Key Laboratory Research Project of Shaanxi Province (No. 17JS085).

References

- [1] J.Q. Luo, B. Zeuner, S.T. Morthensen, A.S. Meyer, M. Pinelo, Separation of phenolic acids from monosaccharides by low-pressure nanofiltration integrated with laccase pre-treatments, *J. Membr. Sci.*, 482 (2015) 83–91.
- [2] Y.H. Tang, Y.K. Lin, B. Zhou, X.L. Wang, PVDF membranes prepared via thermally induced (liquid–liquid) phase separation and their application in municipal sewage and industry wastewater for water recycling, *Desal. Wat. Treat.*, 57 (2016) 22258–22276.
- [3] W.X. Zhang, L.H. Ding, J.Q. Luo, M.Y. Jaffrin, B. Tang, Membrane fouling in photocatalytic membrane reactors (PMRs) for water and wastewater treatment: a critical review, *Chem. Eng. J.*, 302 (2016) 446–458.
- [4] L. Wang, B. Cao, K. Pan, Preparation of hydrophilic poly(vinylidene fluoride) hollow fiber oil/water separation membrane, *Polym. Mater. Sci. Eng.*, 31 (2015) 149–153.
- [5] X.T. Hong, Y.M. Zhou, Z.L. Ye, H.F. Zhuang, W.P. Liu, K.S. Hui, Z. Zeng, X.H. Qiu, Enhanced hydrophilicity and antibacterial activity of PVDF ultrafiltration membrane using $\text{Ag}_3\text{PO}_4/\text{TiO}_2$ nanocomposite against *E. coli*, *Desal. Wat. Treat.*, 75 (2017) 26–33.
- [6] G.B. Guo, S.L. An, S.S. Kou, Preparation and performance of modified poly(vinylidene fluoride) grafted onto a blended polystyrene sulfonated acid membrane, *Acta Phys. Chim. Sin.*, 25 (2009) 2161–2166.
- [7] J. Zhang, Z. Xu, W. Mai, C. Min, B. Zhou, M. Shan, Y. Li, C. Yang, Z. Wang, X. Qian, Improved hydrophilicity, permeability, antifouling and mechanical performance of PVDF composite ultrafiltration membranes tailored by oxidized low-dimensional carbon nanomaterials, *J. Mater. Chem. A*, 1 (2013) 3101–3111.
- [8] A. Ghaee, B. Sadatnia, M. Khosravi, Z. Mansourpour, A. Ghadimi, Preparation and characterization of modified PVDF membrane induced by argon plasma with enhanced antifouling property, *Desal. Wat. Treat.*, 64 (2017) 72–80.

- [9] F. Liu, B.K. Zhu, Y.Y. Xu, Improving the hydrophilicity of poly(vinylidene fluoride) porous membranes by electron beam initiated surface grafting of AA/SSS binary monomers, *Appl. Surf. Sci.*, 253 (2006) 2096–2101.
- [10] M. Obaid, H.O. Mohamed, A.S. Yasin, M.A. Yassin, O.A. Fadali, H.Y. Kim, N.A.M. Barakat, Under-oil superhydrophilic wetted PVDF electrospun modified membrane for continuous gravitational oil/water separation with outstanding flux, *Water Res.*, 123 (2017) 524–535.
- [11] K. Dutta, S. Das, P.P. Kundu, Low methanol permeable and highly selective membranes composed of pure and/or partially sulfonated PVDF-co-HFP and polyaniline, *J. Membr. Sci.*, 468 (2014) 42–51.
- [12] A. Venault, Y.H. Liu, J.R. Wu, H.S. Yang, Y. Chang, J.Y. Lai, P. Aimar, Low-biofouling membranes prepared by liquid-induced phase separation of the PVDF/polystyrene-*b*-poly (ethylene glycol) methacrylate blend, *J. Membr. Sci.*, 450 (2014) 340–350.
- [13] N. Li, C.F. Xiao, S.L. An, X.Y. Hu, Preparation and properties of PVDF/PVA hollow fiber membranes, *Desalination*, 250 (2010) 530–537.
- [14] J. Qiu, L. Zhao, M. Zhai, J. Ni, H. Zhou, J. Peng, J. Li, G. Wei, Pre-irradiation grafting of styrene and maleic anhydride onto PVDF membrane and subsequent sulfonation for application in vanadium redox batteries, *J. Power Sources*, 177 (2008) 617–623.
- [15] E.E. Abdel-Hady, M.O. Abdel-Hamed, S. Awad, M.F.M. Hmamm, Characterization and evaluation of commercial poly(vinylidene fluoride)-*g*-sulfonated Polystyrene as proton exchange membrane, *Polym. Adv. Technol.*, 29 (2018) 130–142.
- [16] H.C. Yang, J.Q. Luo, Y. Lv, P. Shen, Z.K. Xu, Surface engineering of polymer membranes via mussel-inspired chemistry, *J. Membr. Sci.*, 483 (2015) 42–59.
- [17] W.C. Chong, E. Mahmoudi, Y.T. Chung, M.M. Ba-Abbad, C.H. Koo, A.W. Mohammad, Polyvinylidene fluoride membranes with enhanced antibacterial and low fouling properties by incorporating ZnO/rGO composites, *Desal. Wat. Treat.*, 96 (2017) 12–21.
- [18] Z.L. Cui, E. Drioli, Y.M. Lee, Recent progress in fluoropolymers for membranes, *Prog. Polym. Sci.*, 39 (2014) 164–198.
- [19] F. Liu, N.A. Hashim, Y. Liu, M.R.M. Abed, K. Li, Progress in the production and modification of PVDF membranes, *J. Membr. Sci.*, 375 (2011) 1–27.
- [20] A. Rahimpour, S.S. Madaeni, S. Zereshki, Y. Mansourpanah, Preparation and characterization of modified nano-porous PVDF membrane with high antifouling property using UV photo-grafting, *Appl. Surf. Sci.*, 255 (2009) 7455–7461.
- [21] H. Shi, Y. He, Y. Pan, H. Di, G. Zeng, L. Zhang, C. Zhang, A modified mussel-inspired method to fabricate TiO₂ decorated superhydrophilic PVDF membrane for oil/water separation, *J. Membr. Sci.*, 506 (2016) 60–70.
- [22] M.S. Islam, J.R. McCutcheon, M.S. Rahaman, A high flux polyvinyl acetate-coated electrospun nylon 6/SiO₂ composite microfiltration membrane for the separation of oil-in-water emulsion with improved antifouling performance, *J. Membr. Sci.*, 537 (2017) 297–309.
- [23] W. Li, X. Qiu, Study on the structure and morphology of the PVDF-*g*-PSSA membrane prepared by solution graft, *J. Funct. Polym.*, 17 (2004) 452–456.
- [24] J. Byun, J. Sauk, H. Kim, Preparation of PVDF/PSSA composite membranes using supercritical carbon dioxide for direct methanol fuel cells, *Int. J. Hydrogen Energy*, 34 (2009) 6437–6442.
- [25] C. Li, L. Wang, X.D. Wang, M.X. Kong, Q. Zhang, G.Y. Li, Synthesis of PVDF-*g*-PSSA proton exchange membrane by ozone-induced graft copolymerization and its application in microbial fuel cells, *J. Membr. Sci.*, 527 (2017) 35–42.
- [26] Y. Wang, J. Peng, J. Li, M. Zhai, PVDF based ion exchange membrane prepared by radiation grafting of ethyl styrenesulfonate and sequent hydrolysis, *Radiat. Phys. Chem.*, 130 (2017) 252–258.
- [27] G.J. Ross, J.F. Watts, M.P. Hill, Surface modification of poly(vinylidene fluoride) by alkaline treatment 1. The degradation mechanism, *Polymer*, 41 (2000) 1685–1696.
- [28] G.J. Ross, J.F. Watts, M.P. Hill, Surface modification of poly(vinylidene fluoride) by alkaline treatment Part 2. Process modification by the use of phase transfer catalysts, *Polymer*, 42 (2001) 403–413.
- [29] X. Yu, S. Kou, Q. Yang, Y. Zhao, Y. Wei, B. Yao, Study on the preparation and properties of Cu(II) molecularly imprinted membrane (Cu(II)/MIM/PVDF), *Desal. Wat. Treat.*, 85 (2017) 25–35.
- [30] G.D. Kang, H.J. Yu, Z.G. Liu, Y.M. Cao, Surface modification of a commercial thin film composite polyamide reverse osmosis membrane by carbodiimide-induced grafting with poly(ethylene glycol) derivatives, *Desalination*, 275 (2011) 252–259.
- [31] S. Singha, T. Jana, Effect of composition on the properties of PEM based on ploybenzimidazole and ploy (vinylidene fluoride) blends, *Polymer*, 55 (2014) 594–601.
- [32] J. Albo, J. Wang, T. Tsuru, Gas transport properties of interfacially polymerized polyamide composite membranes under different pre-treatments and temperatures, *J. Membr. Sci.*, 449 (2014) 109–118.
- [33] J. Albo, H. Hagiwara, H. Yanagishita, K. Ito, T. Tsuru, Structural characterization of thin-film polyamide reverse osmosis membranes, *Ind. Eng. Chem. Res.*, 53 (2014) 1442–1451.
- [34] C.Q. Xu, W. Huang, X. Lu, D. Yan, S.T. Chen, H. Huang, Preparation of PVDF porous membranes by using PVDF-*g*-PVP powder as an additive and their antifouling property, *Radiat. Phys. Chem.*, 81 (2012) 1763–1769.
- [35] Z.W. Song, L.Y. Jiang, Optimization of morphology and performance of PVDF hollow fiber for direct contact membrane distillation using experimental design, *Chem. Eng. Sci.*, 101 (2013) 130–143.
- [36] D.J. Kim, H.J. Lee, S.Y. Nam, Sulfonated poly(arylene ether sulfone) membranes blended with hydrophobic polymers for direct methanol fuel cell applications, *Int. J. Hydrogen Energy*, 59 (2013) 189–199.
- [37] D.J. Kim, H.Y. Hwang, S.B. Jung, S.Y. Nam, Sulfonated poly(arylene ether sulfone)/laponite-SO₃H composite membrane for direct methanol fuel cell, *J. Ind. Eng. Chem.*, 18 (2012) 556–562.
- [38] M.F. Rabuni, N.M. Nik Sulaiman, N. Awanis Hashim, A systematic assessment method for the investigation of the PVDF membrane stability, *Desal. Wat. Treat.*, 57 (2016) 1–12.
- [39] A.J. Lovinger, Annealing of poly(vinylidene fluoride) and formation of a fifth phase, *Macromolecules*, 15 (1982) 40–44.
- [40] N. Awanis Hashim, Y. Liu, K. Li, Stability of PVDF hollow fibre membranes in sodium hydroxide aqueous solution, *Chem. Eng. Sci.*, 66 (2011) 1565–1575.
- [41] D. Rana, Y. Kim, T. Matsuura, H.A. Arafat, Development of antifouling thin-film composite membranes for seawater desalination, *J. Membr. Sci.*, 367 (2011) 110–118.
- [42] R. Jamshidi Gohari, E. Halakoo, N.A.M. Nazri, W.J. Lau, T. Matsuura, A.F. Ismail, Improving performance and antifouling capability of PES UF membranes viablending with highly hydrophilic hydrous manganese dioxide nanoparticles, *Desalination*, 335 (2014) 87–95.
- [43] J.F. Kim, J.T. Jung, H.H. Wang, S.Y. Lee, T. Moore, A. Sanguineti, E. Drioli, Y.M. Lee, Microporous PVDF membranes via thermally induced phase separation (TIPS) and stretching methods, *J. Membr. Sci.*, 509 (2016) 94–104.
- [44] D.P. Liu, J. Zhu, M. Qiu, C.J. He, Antifouling performance of poly(lysine methacrylamide)-grafted PVDF microfiltration membrane for solute separation, *Sep. Purif. Technol.*, 171 (2016) 1–10.
- [45] S. Ayyaru, Y.-H. Ahn, Application of sulfonic acid group functionalized graphene oxide to improve hydrophilicity, permeability, and antifouling of PVDF nanocomposite ultrafiltration membranes, *J. Membr. Sci.*, 525 (2017) 210–219.
- [46] S. Yu, X. Zhang, F. Li, X. Zhao, Poly(vinyl pyrrolidone) modified poly(vinylidene fluoride) ultrafiltration membrane via a two-step surface grafting for radioactive wastewater treatment, *Sep. Purif. Technol.*, 194 (2018) 404–409.
- [47] L. Zhang, Z. Shu, N. Yang, B. Wang, H. Dou, N. Zhang, Improvement in antifouling and separation performance of

- PVDF hybrid membrane by incorporation of room-temperature ionic liquids grafted halloysite nanotubes for oil–water separation, *J. Appl. Polym. Sci.*, 135 (2018) 46278.
- [48] L. Wang, K. Pan, L. Li, B. Cao, Surface hydrophilicity and structure of hydrophilic modified PVDF membrane by nonsolvent induced phase separation and their effect on oil/water separation performance, *Ind. Eng. Chem. Res.*, 53 (2014) 6401–6408.
- [49] S. Wang, L.Y. Chu, W.M. Chen, X.C. Xiao, G.J. Wang, Advances in researches on oil/water separation membranes, *Oilfield Chem.*, 20 (2003) 387–390.
- [50] L. Nord, B. Karlberg, Extraction based on the flow-injection principle: Part 5. Assessment with a membrane phase separator for different organic solvents, *Anal. Chim. Acta*, 118 (1980) 285–292.
- [51] C.S. Ong, W.J. Lau, P.S. Goh, A.F. Ismail, B.C. Ng, Preparation and characterization of PVDF-PVP-TiO₂ composite hollow fiber membranes for oily wastewater treatment using submerged membrane system, *Desal. Wat. Treat.*, 50 (2013) 1–11.